Available online at www.sciencedirect.com

ScienceDirect

www.elsevier.com/locate/jes

JES JOURNAL OF ENVIRONMENTAL SCIENCES

www.jesc.ac.cn

Temporal variability of visibility and its parameterizations in Ningbo, China

Jingjing Zhang[1,2,3,**], *Lei Tong*[1,2,**], *Chenghui Peng*[2,3], *Huiling Zhang*[2,3], *Zhongwen Huang*[4], *Jun He*[5], *Hang Xiao*[1,2,*]

1. *Center for Excellence in Regional Atmospheric Environment, Institute of Urban Environment, Chinese Academy of Sciences, Xiamen 361021, China*
2. *Key Lab of Urban Environment and Health, Institute of Urban Environment, Chinese Academy of Sciences, Xiamen 361021, China*
3. *University of Chinese Academy of Sciences, Beijing 100049, China*
4. *School of Chemistry and Environmental Engineering, Hanshan Normal University, Chaozhou 521041, China*
5. *International Doctoral Innovation Center, Department of Chemical and Environmental Engineering, University of Nottingham Ningbo China, Ningbo 315830, China*

ARTICLE INFO

Article history:
Received 22 March 2018
Revised 12 September 2018
Accepted 13 September 2018
Available online 26 September 2018

Keywords:
Visibility
Multiple correspondence analysis (MCA)
Multiple non-linear regression

ABSTRACT

Simultaneous and continuous measurements of visibility, meteorological parameters and air pollutants were carried out at a suburban site in Ningbo from June 1, 2013 to May 31, 2015. The characteristics of visibility and their relationships with air pollutants and meteorological factors were investigated using multiple statistical methods. Daily visibility ranged from 0.6 to 34.1 km, with a mean value of 11.8 km. During the 2-year experiment, 43.4% of daily visibility was found to be less than 10.0 km and only 9.2% was greater than 20.0 km. Visibility was lower in winter with a frequency of 53.4% in the range of 0.0–5.0 km. Annual visibility had an obvious diurnal variation, with the lowest and highest visibility being 7.5 km at approximately 06:00 local time and 15.6 km at approximately 14:00 local time, respectively. Multiple correspondence analysis (MCA) indicated that the different ranges of visibility were significantly affected by different levels of pollutants and meteorological conditions. Based on the analyses, visibility was found to be an exponential function of $PM_{2.5}$ concentrations within a certain range of relative humidity. Thus, non-linear models combining multiple linear regressions with exponential regression were subsequently developed using the data collected from June 2014 to May 2015, and the data from June 2013 to May 2014 was used to evaluate the performance of the model. It was demonstrated that the derived models can quantitatively describe the relationships between visibility, air quality and meteorological parameters in Ningbo.

* *Corresponding author.*
E-mail: hxiao@iue.ac.cn. (H. Xiao).
** The authors contributed equally to this article.

https://doi.org/10.1016/j.jes.2018.09.015
1001-0742 © 2018 The Research Center for Eco-Environmental Sciences, Chinese Academy of Sciences. Published by Elsevier B.V.

Introduction

Horizontal visibility is defined as the greatest distance at which a black object can be visually identified with unaided eyesight against a light sky (Wark et al., 1998; Watson, 2002). The reduction of atmospheric visibility is an important indicator of deteriorating ambient air quality in the absence of unusual weather. Visibility degradation has become a serious environmental issue of public concern in populated cities and has been reported to have adverse effects on human health, crop growth and traffic safety (Che et al., 2006). It has been widely confirmed that the impairment of visibility is mainly due to the scattering and absorption of visible light by suspended particles (Chan et al., 1999; Horvath, 1995).

Atmospheric particulate matter (PM) is associated with both anthropogenic and natural emissions that consist of minuscule particles of solid or liquid matter, with diameters ranging from 0.01 to 100 μm. Atmospheric particles can affect the climate by both direct and indirect radiative forcing (Charlson et al., 1992; Xu et al., 2002), especially fine aerosols with aerodynamic diameters of 2.5 μm or less ($PM_{2.5}$). Particles of decreasing size will remain suspended in the atmosphere for longer and subsequently impact the environment over greater distances. $PM_{2.5}$, which comprise sulfates, nitrates, organic and elemental carbon, could effectively scatter or absorb visible light and thus reduce visibility (Zhang et al., 2012; Kim et al., 2006; Tan et al., 2009a, 2009b). All these airborne particles, together with other gaseous pollutants such as sulfur dioxide (SO_2) and nitrogen dioxides (NO_2) could contribute to the increase of haze and lead to a low visual range (≤10 km). Specifically, the heterogeneous aqueous transformation from SO_2 and NO_2 is enhanced during haze episodes, which probably leads to the remarkable secondary formation of sulfate and nitrate in fine particles, further impairing visibility (Wang et al., 2006). In addition to air pollutants, many meteorological parameters such as relative humidity (RH), wind speed (WS), wind direction (WD), temperature (T), pressure and precipitation can also contribute to light extinction and degrade air quality (Zhao et al., 2011; Yang et al., 2007). In haze events, the rapid increase of PM concentrations, high RH, and low WS, can adversely impact atmospheric visibility (Tsai 2005; Zhang et al., 2010; Deng et al., 2011). As RH increases, hygroscopic particles progressively absorb more moisture, which will increase the scattering cross section of aerosols and proportionately reduce visibility. Therefore, RH could directly affect the particles that contribute to visibility reduction. While other meteorological variables such as WS, temperature, and pressure have indirect effects on visibility, they may also affect the concentration of atmospheric particles due to thermal and mechanical turbulence (Du et al., 2013). The accumulation and transport of particles are closely related to the synoptic systems and atmospheric circulations. Some studies have identified that high atmospheric pressure, low WS, high RH and low mixing layer height could significantly reduce visibility in Taiwan and Nanjing (Tsai, 2005; Deng et al., 2011).

The forecasting and early warning of visibility is not only important to environment and public health, but also to traffic control and even military actions. A number of models were previously developed to describe the correlations between visibility and air pollution, and continuous efforts have been made to improve the models based on the monitoring results of visibility measurements. Multiple linear regression equations have been established to investigate the effect of air pollutants and meteorological conditions on visibility in Taiwan (Wen and Yeh, 2010). In addition, different empirical regression models were developed for visibility in Beijing, Shanghai and Guangzhou, with a logarithm of coarse particle concentration used in the regression analyses (Lin et al., 2012; Tsai, 2005). Additionally, several studies have suggested that visibility is a linear response to the exponential function of $PM_{2.5}$ concentrations under a certain RH range (Cao et al., 2012; Yu et al., 2016; Shen et al., 2016). All these studies suggested that the impacts of air quality and other variables on visibility are more complicated than linearity. However, there is still a lack of research on the characteristics of visibility in the Ningbo area, and its relationship with air pollutants and meteorological conditions.

Ningbo, is the second largest city of Zhejiang Province, and has experienced a severe loss of visibility in recent decades (Zhang et al., 2012). In this study, visibility was monitored from June 2013 to May 2015, with the potential relationships between visibility, air pollutants, and meteorological variables being investigated. The objectives of this study were (1) to characterize the temporal variations of visibility in the suburb of Ningbo; (2) to identify the relationships between classified visibility and other parameters using multiple correspondence analysis (MCA); (3) to provide new knowledge for improving visibility prediction in the Ningbo region.

1. Material and methods

1.1. Study area and data source

Ningbo (28°51′–30°33′ N, 120°55′–122°16′ E) is a coastal city of the Zhejiang Province in Eastern China. The city lies in the south of Hangzhou Bay and faces the East China Sea with an area of 9816 km^2. The climate conditions of Ningbo are governed by the sub-tropical monsoon, with prevailing northwest and southeast winds in winter and summer, respectively. The annual mean air temperature and precipitation are 16.4 °C and 1480 mm, respectively. Annual mean air temperature reaches its maximum (28.0 °C) in July and minimum (4.7 °C) in January. During the whole year, approximately 60% of the annual mean precipitation occurs from May to September. The annual mean WS is 2–3 m/sec in urban areas and > 5 m/sec in coastal areas.

Ningbo is one of the most highly urbanized and industrialized cities in the Yangtze River Delta (YRD) region and had a population of 7.87 million people and a vehicle fleet of 1.98 million in September 2016. With a rapid urbanization and an increase in motor vehicle numbers, energy consumption in Ningbo has increased substantially and haze events have been frequently observed in recent years (He et al., 2016; Cheng et al., 2014; Hua et al., 2015). Air pollutant concentrations and meteorological data from June 1, 2013 to May 31, 2015 at the Dongqian Lake (DQL) Monitoring Station (29°45′N, 121°37′E) were collected in this study. The monitoring station is 12 km away from the city centre of Ningbo and 1.3 km from the largest

freshwater lake (Dongqian Lake, 22 km^2 in area) in the Zhejiang Province. There are several hills nearby to the west and east. Many small villages are distributed at the foot of the mountain less than 2 km to DQL site. There is a provincial road close to this site with small factories involved in mechanical processing built alongside. In recent years, the number of tourists visiting near the DQL site have also increased.

The DQL station is a part of the national air quality monitoring network of China, which is under the supervision of the national Ministry of Environmental Protection (MEP). Visibility is measured by trained operators using easily identifiable structures and objects, such as tall buildings, towers, and mountain ridges, at predetermined distances. The routine monitoring of air quality using six criteria air pollutants, i.e. SO_2, NO_2, carbon monoxide (CO), ozone (O_3), particulate matter with aerodynamic diameters of 10 μm or less (PM_{10}), $PM_{2.5}$ at DQL station began in 2012 when the latest ambient air quality standards of China (GB 3095-2012) were established. Commercial instruments from Thermo-Fisher Scientific Inc. (USA) are used to measure gaseous pollutants, such as O_3 (Model 49i), NO_2 (Model 42i), CO (Model 48i) and SO_2 (Model 43i). $PM_{2.5}$ and PM_{10} are measured using a tapered-element oscillating microbalance sampler (R&P TEOM, 1400). The TEOM sampler is calibrated regularly using filters with measured masses. Zero and span checks are made weekly. Hourly averaged data were used for all analyses in this study and described by local time (UTC + 8). Meteorological variables including RH, WS, temperature, and atmospheric pressure are measured by automatic weather station (WS500-UMB, Lufft, Germany) at the DQL site.

The Air Quality Index (AQI) has been developed to provide daily air quality information to the public in China (Zheng et al., 2014). On February 29, 2012, the MEP of the People's Republic of China (PRC) approved the technical regulation on ambient air quality index (GB 3095–2012), which released $PM_{2.5}$ values and calculated the AQI instead of the Air Pollution Index (API). A sub-index is calculated for each pollutant from a segmented linear function that transforms ambient concentrations onto a scale from 0 to 500. AQI is calculated as the sub-index maximum (China's Environmental Protection Standards, HJ 633-2012). Daily AQI is defined as:

$$AQI = \max\left(AQI_{PM10}, AQI_{PM2.5}, AQI_{SO2}, AQI_{NO2}, AQI_{CO}, AQI_{O3}\right) \quad (1)$$

where AQI_{PM10}, $AQI_{PM2.5}$, AQI_{SO2}, AQI_{NO2}, AQI_{CO} and AQI_{O3} are the partial index of air pollutants PM_{10}, $PM_{2.5}$, SO_2, NO_2, CO and O_3, respectively.

$$AQI_p = \left[\left(AQI_{ph} - AQI_{pl}\right)/\left(C_{high} - C_{low}\right)\right] \times \left(C_p - C_{low}\right) + AQI_{pl} \quad (2)$$

where AQI_p is the partial index of air pollutant p, C_p is the daily average concentration of air pollutant p, and C_{high} and C_{low} are the threshold concentrations of p at air quality grade. Corresponding to C_{high} and C_{low}, AQI_{ph} and AQI_{pl} are the threshold partial indexes of air pollutant p at air quality grade, respectively.

1.2. Data analysis

MCA is a data analysis technique for categorical data, used to detect and represent the underlying structures in a data set (Hair et al., 1995; Hill and Lewicki, 2007). The results of MCA can imply that objects within the same category are plotted close to each other and objects in different categories are plotted as far apart as possible. This statistical method has been widely used in sociology, economic statistics, medical science, but is still limited in environmental science (Van Stan et al., 2016; Sourial et al., 2010). In addition, all air pollutants and meteorological data were carried out using a multiple linear regression (MLR) analysis incorporating a stepwise method to develop empirical models in Ningbo. The above statistical analyses were performed using SPSS software (Version 22.0 for Windows, IBM Inc.)

2. Results and discussion

2.1. Descriptive results

The overall statistical analysis of daily visibility, air pollutants, and meteorological variables during the two years of observations at DQL station are summarized in Table S1. Day-to-day variations of visibility, $PM_{2.5}$ and PM_{10} are shown in Fig. S1. From June 1, 2013 to May 31, 2015, the daily average visibility ranged from 0.6 to 34.1 km, with a mean value of 11.8 km, which was just over the defined threshold for haze (i.e. visibility <10.0 km), indicating poor air quality over the study region. The mean $PM_{2.5}$, PM_{10}, SO_2, NO_2, CO and O_3 concentrations were 42.6, 64.6, 15.0, 28.9, 0.9 and 70.2 μg/m^3, respectively. The average value of AQI, RH, temperature, WS and surface pressure were 65.6, 73.2%, 17.8 °C, 1.7 m/sec and 1013.0 hPa, respectively.

Visibility impairment mainly resulted from airborne particulate matter, particularly from $PM_{2.5}$ (Deng et al., 2014; Sabetghadam and Ahmadi-Givi 2014). According to the air quality daily report from MEP, $PM_{2.5}$ in the atmosphere was the primary pollutant of concern in Ningbo during the two years of monitoring (http://www.zhb.gov.cn/hjzl/zghjzkgb/lnzghjzkgb/). Therefore, the daily variations of PM_{10} and $PM_{2.5}$ were required for analysis during the study period in DQL station. Fig. S1 shows that the concentrations of $PM_{2.5}$ and PM_{10} were generally higher in winter and lower in summer, and the proportion of $PM_{2.5}$ in PM_{10} was relatively high. During the two years, almost all daily $PM_{2.5}$ concentrations in winter exceeded the national ambient air quality standard Grade II (75 μg/m^3) (China Environmental Protection Ministry 2012), revealing severe pollution from fine particles. In December, 2013, extremely high levels of PM_{10} and $PM_{2.5}$ were observed with daily average concentrations of 511 and 389 μg/m^3, respectively. At 22:00 on December 6, the hourly concentrations of PM_{10} and $PM_{2.5}$ reached peak values of 707 and 530 μg/m^3, respectively. Visibility dramatically decreased to 0.6 km during this episode, which was the minimum value measured during the two years. This haze episode was also observed in the YRD region (Xue et al., 2015).

2.2. Seasonal and diurnal variations of visibility

Fig. 1a shows that 43.4% of the daily visibility was less than 10.0 km during the two years and only 9.2% was greater than

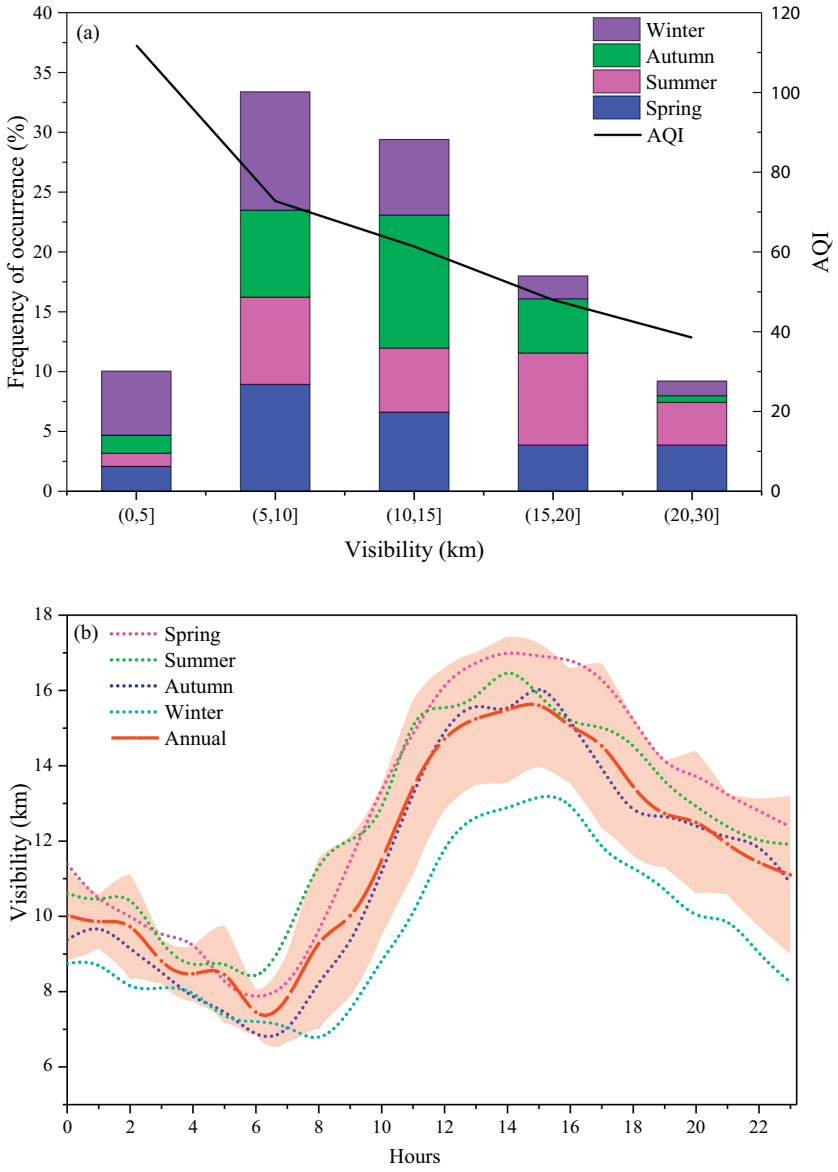

Fig. 1 – Distribution of frequency of occurrence of daily visibility (a), and diurnal variations of annual and seasonal visibility (b) at DQL in Ningbo. The shading area shows the standard deviations for the annual data.

20.0 km, indicating bad air quality in the DQL area. The maximal frequency (33.4%) of daily visibility was observed in the range of 5.0–10.0 km. Poor visibility (<5.0 km) often occurred in winter with a frequency of 53.4%. Daily visibilities of spring and summer contributed as much as 41.8% and 38.8% to the visual range of 20.0–35.0 km, respectively.

Generally, the average value of AQI decreased with increasing visibility (Fig. 1). The mean value of AQI for the visual range of 0–5.0 km was 111.8 (≥100), which indicates the occurrence of a haze episode under low visibility. The AQI values were 72.3 and 61.4 for the visual range of 5.0–10.0 km and 10.0–15.0 km, respectively. This indicates that the local air was moderately polluted. Good visibility (15.0–35.0 km) occurred simultaneously with the lowest AQI value (<50), i.e. when the air quality was good. These data confirmed that the local air quality had an obvious positive correlation with visibility (Tsai et al., 2003).

Fig. 1b depicts the diurnal patterns of annual and seasonal mean visibility in Ningbo. Visibility shows an obvious and similar diurnal variation throughout four seasons, with a sharp decrease in early morning, i.e. 06:00–08:00 local time and a peak in the afternoon, i.e. 14:00–16:00 local time. From the perspective of the annual average, the lowest and highest visibility was 7.5 and 15.6 km, respectively. The diurnal patterns during different seasons were desynchronized, which is due to differences in weather pattern (i.e. day-night length, sunrise and sunset time, monsoon etc.) and the stability of atmospheric boundary layer (ABL) in each season. For example, the lowest and highest daily levels of visibility in wintertime are nearly two hours later than in summertime,

which is mainly attributed to a later sunrise time and smaller ABL depth. It can also be seen that visibility in spring and summer was better than in autumn and winter, with winter more associated with poor visibility and bad air quality.

2.3. Monthly variations of visibility and environmental factors

Monthly variations of visibility, air pollutant concentrations and meteorological factors were investigated in this study (Fig. 2). The highest average visibility was observed in July, with a value of 16.6 km, and the lowest average visibility was observed in December with a value of 9.1 km. Different trends of monthly variations were observed between visibility and other environmental variables in the study area. It was noteworthy that the visibility greatly decreased in June, when the air pollutant concentrations stayed at low levels. It is well-known that visibility is negatively correlated with air humidity (Deng et al., 2011). The relatively high level of RH in June might account for the lower visibility due to the light scattering and absorption of water vapor.

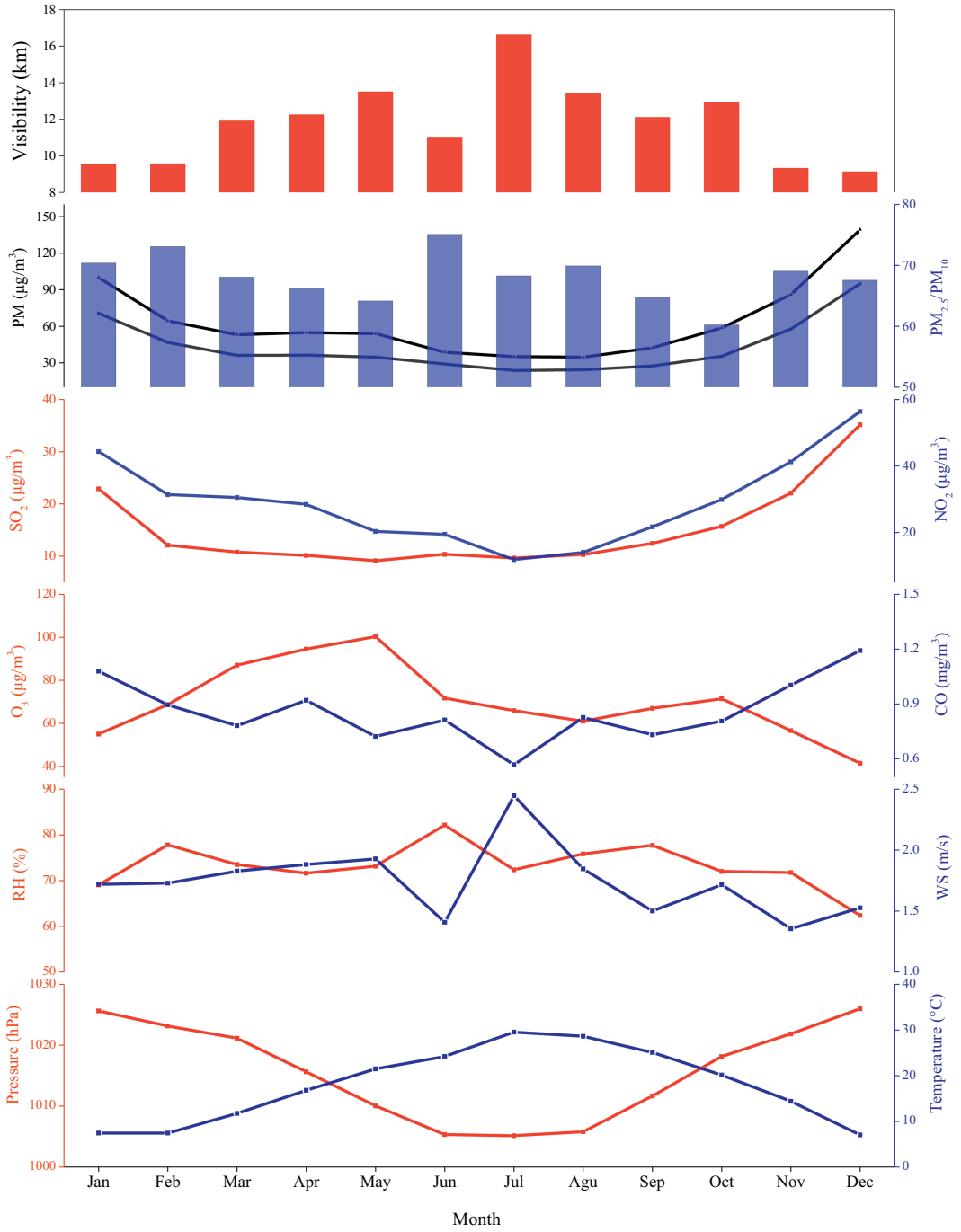

Fig. 2 – Monthly variations of visibility and other environmental variables.

Fig. 2 shows that the PM_{10} and $PM_{2.5}$ pollution of the study area was severe. The monthly mass concentrations of PM_{10} and $PM_{2.5}$ were in the range of 34.7–139.3 and 23.7–94.9 $\mu g/m^3$, respectively. The concentrations of PM_{10} and $PM_{2.5}$ were higher from November to February, while lower from June to September. The temporal variations of anthropogenic emissions and weather conditions might account for the seasonal cycle of PM. The average ratio of $PM_{2.5}$ to PM_{10} (i.e. $PM_{2.5}/PM_{10}$) was 66.6% with a range of 59.3%–72.1%. Remarkably, there was a negative correlation (−0.47, $P < 0.001$) between visibility and $PM_{2.5}/PM_{10}$ (Table S4), especially in June, July and October. The high proportions of $PM_{2.5}$ contained within PM_{10} in poor visibility episodes indicated that fine particles could play an important role in affecting local visibility.

The monthly variations of SO_2, NO_2 and CO were consistent with PM which could also be confirmed by Pearson correlation, with higher and lower concentrations being observed in winter and summer, respectively. All three gaseous pollutants showed negative correlations with visibility (Table S4). However, the observed correlation between O_3 and visibility can be related to the observation that O_3 concentration is typically higher in summer, and positively associated with temperature (Fig. 2). Two monthly peaks of O_3 were observed in May (100.3 $\mu g/m^3$) and October (71.4 $\mu g/m^3$) along with better visibility, while the lowest O_3 concentration (41.4 $\mu g/m^3$) occurred in December when lower visibility was observed. The winter minimum O_3 level is commonly observed in mid-latitude locations in the Northern Hemisphere (Tu et al., 2007; Semple et al., 2012; Kumar et al., 2010), which is mainly due to the relatively weaker photochemical processes. Good visibility is often related to stronger solar radiation, which can significantly promote the photochemical generation of O_3 (Pudasainee et al., 2006). This might account for the good correlation between O_3 levels and visibility during warm seasons in this study.

The variation of RH displayed a summer maximum and winter minimum, with the highest (82.1%) and lowest (62.3%) values occurring in June and December, respectively. A negative correlation (−0.452) between visibility and RH was observed together with a positive correlation (0.358) between $PM_{2.5}/PM_{10}$ and RH (Table S4). With an increase of RH, the generation of secondary aerosols in fine particles was enhanced and the hygroscopic components of aerosols such as sulfate, nitrate and sea salt absorbed more moisture, which would increase the scattering cross section of the aerosols and reduce visibility (Jung et al., 2009).

Obvious monthly variations of surface WS were observed in the study area, with the highest value (2.4 m/sec) occurring in July and the lowest value (1.4 m/sec) occurring in November (Fig. 2). Monthly visibility was positively correlated with WS during most months, especially in summer (June–August) and autumn (September–November). Generally, the increase of WS accelerates the diffusion of dust and pollutants, which leads to an increase of the visual range. Meanwhile, the temperature and pressure also expectedly changed between different months. Temperature was highest (29.5 °C) in July and lowest (7.0 °C) in December, while the barometric pressure was highest (1025.9 hPa) in December and lowest (1005.1 hPa) in July. In general, the variation of visibility was consistent with that of temperature and opposite to that of pressure. The correlations between visibility and temperature and pressure might be accounted for by the following reasons. High air temperature and low pressure usually enhance the dispersal capability of the atmosphere via thermal and mechanical turbulence, which could promote the improvement of air quality and visibility and inversely, low temperature and high pressure indicate more stable weather conditions, which would weaken the diffusion of air pollutants.

2.4. Multiple correspondence analysis of visibility

In MCA, all variables were divided into four categories according to magnitude (Table S2). Specifically, values 1 to 4 were used to represent small to large, respectively, with the category indicator added as a prefix for air pollution, and the suffix describing the meteorological parameter. The correspondence plot and loading factors of visibility and other environmental variables based on MCA are shown in Fig. 3 and Table S3, respectively. Most of the variance in our data was accounted for in the analysis with axes 1 and 2 explaining 41.5% and 25.4% variation, respectively. Almost all air pollutants and meteorological factors were classified into four quadrants in the plot. The relative distance between variables and the closeness of points on the plot with respect to their angle from the origin, and points in the same quadrant can be used to interpret relationships between variables (Higgs, 1991; Garson, 2012). The origin on the plot corresponds to the centroid of each variable. The closer a variable is to the origin, the closer it is to the average profile. Fig. 3 shows that V2 and V3 were near to the origin and were the main visual range during study period. The frequency of daily visibility appearing in the range of 5.0–15.0 km was higher than those of others (Fig. 1). In addition, $4NO_2$, 4CO and $4SO_2$ were located far from the origin in the first quadrant and therefore had the greater variability. This implied that the concentration of air pollutants had the greatest effect compared to other factors during the poor visual range (V1 < 5 km). Along dimension 2, it was observed that T4, $1PM_{2.5}$, 1CO and WS4 had the most effect, indicating that the lower concentrations of pollutants except for O_3, higher temperature and higher wind speed had a significant influence on good visibility (V4 > 15 km).

Fig. 3 illustrates that the first two dimensions accounted for 66.9% of the total variance and the majority of variables were clearly discriminated in both dimensions. Along dimension 1, values of $PM_{2.5}$, SO_2, CO, NO_2 and P increased positively with the direction of dimension 1. Conversely, T, V and WS decreased in dimension 1. However, only WS along dimension 2 changed regularly, which increased in a positive direction. Generally, dimension 1 could account for most air pollutants, P, T, V and WS with dimension 2 only additionally explaining WS. However, the two dimensions in our analysis did not clearly explain the variations of O_3 and RH, and the lower loading factors of O_3 and RH in Table S3 also confirmed this.

The variation of O_3 concentrations and RH did not regularly change with dimension 1 or 2, indicating that further dimensions may need to be analyzed, i.e. the variation of O_3 has unique characteristics. As previously discussed, visibility was usually positively correlated with O_3 concentrations. $4O_3$

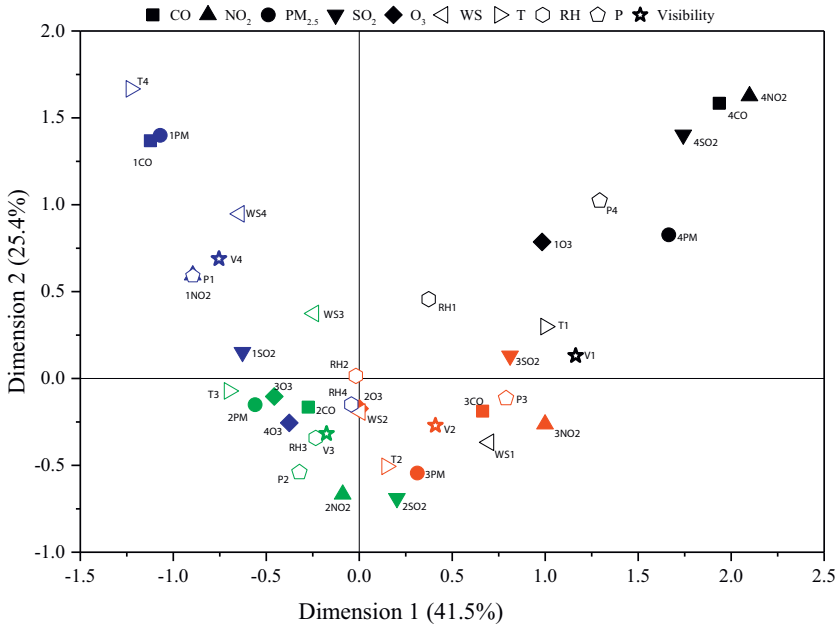

Fig. 3 – Category quantification plot of classified visibility and other environmental variables at DQL.

was closely distributed with V3 rather than V4 in the correspondence map (Fig. 3), but the concentration of O_3 did not increase with visibility completely. In fact, except for the lower concentrations of O_3, the points of $2O_3$ to $4O_3$ were all closely placed within the third quadrants of Fig. 3, which were generally associated with a relatively higher temperature and lower WS. The relatively high WS (WS4 & WS3) in the second quadrant was unfavorable to the accumulation of O_3. These data also indicated that the production of O_3 was not only affected by visibility, other pollutants and meteorological parameters, but also factors including solar radiation, which was not included in this study (Tong et al., 2017). In addition, the effects of RH on visibility could not be ignored. The visibility was always below 15 km (V1~V3) when RH was higher than 80% (i.e. RH3 & RH4), which indicated that visibility remained at low values even with low air pollution concentrations.

2.5. *Relationship between visibility and other factors*

To gain a deeper insight into how relevant factors affect visibility, Pearson correlations were performed between daily visibility, air pollutants and meteorological variables (Table S4). Visibility had significantly negative correlations with $PM_{2.5}$ ($r = -0.50$), CO ($r = -0.51$), and NO_2 ($r = -0.47$). The moderate relationship between visibility and $PM_{2.5}$ was expected, given the scattering effect of aerosols, especially fine particles (Charlson et al., 1992; Xu et al., 2002). Visibility had no direct relationship with CO, but the correlation coefficient between both variables was a little higher than that between visibility and $PM_{2.5}$. This may be because CO is generated by intensive biomass burning together with incomplete combustion from vehicle engines, during which large quantities of particles would be generated. Fine particles formed simultaneously with CO could lead to visibility reduction by scattering and absorbing light radiation (Xue et al., 2015), which might account for the negative correlation between visibility and CO. For NO_2, there was a weak direct influence on visibility. However, secondary pollutants such as nitrate, which is produced by photochemical conversions from NO_2 might play an important role in visibility reduction (Sabetghadam and Ahmadi-Givi, 2014). Nitrate is the main water-soluble constituent in $PM_{2.5}$ and is an important factor in the increase of $PM_{2.5}$ concentrations. A strong positive correlation between NO_2 and $PM_{2.5}$ ($r = 0.70$, Table S4) was observed in this study, which might explain why NO_2 was significantly correlated with visibility in the DQL area.

In analyses examining effects of meteorological factors, visibility showed a significant positive correlation ($r = 0.39$) with WS and a negative correlation ($r = -0.40$) with RH, which was in accordance with previous research (Deng et al., 2011; Zhang et al., 2010). High wind speed would promote the dispersion of pollutants and could reduce air pollutant concentrations and increase visibility. Also, hygroscopic aerosols are greatly increased with high RH, which could cause the increase of PM concentration and extinction capability, further reducing visibility. As presented in Table S4, visibility showed a rather weak negative and positive correlation with air pressure and temperature, respectively. Air pressure and temperature are both important indicators of a weather system at a given location, and they have no direct effect on visibility. The changes of air pressure and temperature could have an impact on the diffusivity of the atmosphere, and further affect the concentration of air pollutants. The relatively high correlation between $PM_{2.5}$ and temperature ($r = -0.45$), and between $PM_{2.5}$ and pressure ($r = 0.43$) also confirmed this conclusion.

Scatter plots and regression functions of one-year data (Fig. 4) were applied in this study in order to examine the deep

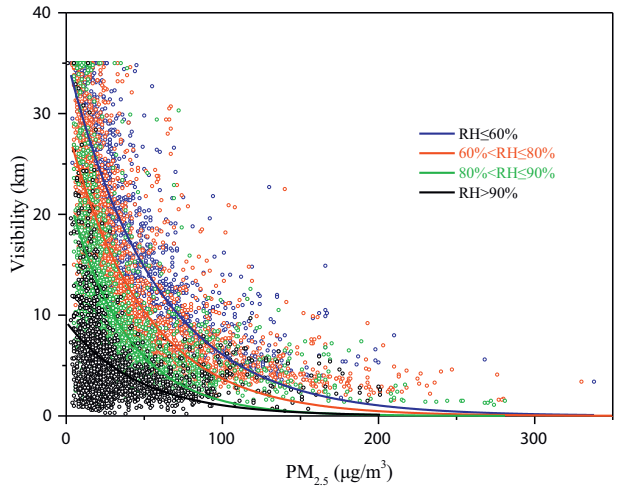

Fig. 4 – Relationships between one-year visibility and $PM_{2.5}$ at DQL (2014.6.1–2015.5.31). Data points are color coded by RH. All the data are hourly average.

connections between visibility and the two major factors (i.e. $PM_{2.5}$ and RH). Fig. 4 and obtained Eq. (3) show the relationships between hourly-averaged visibility and mass concentration of $PM_{2.5}$ under different RH conditions (Yu et al., 2016). RH was classified over four ranges: RH ≤ 60%, 60 < RH ≤ 80%, 80 < RH ≤ 90%, and RH > 90%. The visibility decreased exponentially with increasing $PM_{2.5}$ concentrations in each RH range.

$$\text{Visibility} = f(PM_{2.5}) = \begin{cases} 35.65 \times \exp(-0.017 \times PM_{2.5}), & (RH \le 60\%), r = 0.835 \\ 28.99 \times \exp(-0.020 \times PM_{2.5}), & (60\% < RH \le 80\%), r = 0.732 \\ 22.84 \times \exp(-0.027 \times PM_{2.5}), & (80\% < RH \le 90\%), r = 0.599 \\ 9.32 \times \exp(-0.021 \times PM_{2.5}), & (RH > 90\%), r = 0.384 \end{cases} \quad (3)$$

Firstly, with the increase of $PM_{2.5}$ concentration, the visual range decreased exponentially. Initially, the visibility decreased sharply while the $PM_{2.5}$ concentration increased; but when $PM_{2.5}$ concentrations reached a certain level (e.g. above 100 μg/m^3), the change in visibility was not sensitive to $PM_{2.5}$ concentrations any further. Secondly, with the increase of RH, a lower correlation coefficient between $PM_{2.5}$ and visibility was observed. This implied that visibility stayed at a very low level when RH values were very high (>80%), even with low $PM_{2.5}$ concentrations. In this case, a large amount of water vapor could cover particle surfaces, enhancing the scattering ability of aerosol and reduce visibility significantly. Thirdly, the maximum visibility under different RH conditions was decreased with the increase of RH value (Fig. 4). Eq. (3) suggested that the maximum visibility was just 9.32 km in the case of RH > 90%, and this result was consistent with MCA (Fig. 3).

Obviously, a single parameter regression such as Eq. (3) are not suitable for the forecasting of visibility at another location or in another year, which ignores the effects of other environmental variables, such as NO_2, CO, T, WS etc. As presented in Fig. S2, in which a year's hourly visibility was predicted with Eq. (3), the regression lines between observed and simulated visibility significantly deviate from the 1:1 diagonal line. A larger deviation existed when RH > 90%, indicating a greater contribution of other factors to visibility. Nevertheless, the above equation further confirmed the exponential relationship between visibility and $PM_{2.5}$ under different RH levels. This finding should form the basis of a forecasting model of visibility.

2.6. Regression model development and validation

To further develop a brief model for visibility prediction in Ningbo, it was first assumed that the apparent visibility is the final result of a combination of factors influencing air pollution together with meteorological parameters. As shown in Eq. (4),

$$\text{Visibility} = f(PM_{2.5}) + f(RH, T, NO_2, O_3\cdots) = f(PM_{2.5}) + \sum_i (a_i \cdot x_i) + \varepsilon \quad (4)$$

where x_i represents any important factor for visibility, a_i is a linear regression coefficient, and ε is the error term.

$$\text{Visibility} - f(PM_{2.5}) = \sum_i (a_i \cdot x_i) + \varepsilon \quad (5)$$

or

$$\text{Visibility} - \sum_i (a_i \cdot x_i) = f(PM_{2.5}) + \varepsilon \quad (6)$$

The obtained regression parameters in Eq. (3) were chosen as initial values of modeling fit. Multiple linear regression was conducted between the residue of prediction and other environmental parameters. Datasets with hourly resolution from June 2014 to May 2015 were used to develop the multiple nonlinear regression equations. An independent variable was added into the regression equation by a stepwise procedure based on importance. It demonstrated that for the first two RH categories, i.e. RH ≤ 80%, RH is the common factor in addition to particle concentration for the variation of visibility, then the regression equations for these two levels were eventually combined together. After several circles of regression and iteration, the final modeling results considering main influencing factors besides $PM_{2.5}$ and RH within three RH ranges are listed in Table 1. It showed that the main contributors to visibility under different RH are different, and the influence of all variables on visibility was additive. Specifically, the independent variables in the model are $PM_{2.5}$, and RH when RH ≤ 80%, while O_3 is the major

Table 1 – Regression models of visibility under different RH in DQL, June 2014–May 2015.

Stepwise regression model		Correlation coefficient	N.
V = 23.044 + 27.853*exp.($-0.04199PM_{2.5}$) –0.196RH	RH ≤ 80%	0.816	4247
V = 56.072 + 24.44*exp.($-0.07128PM_{2.5}$) –0.536RH-0.037O_3	80 < RH ≤ 90%	0.671	2049
V = 79.095 + 10.228*exp.($-0.06571PM_{2.5}$) –0.822RH + 0.033 T	RH > 90%	0.589	1697

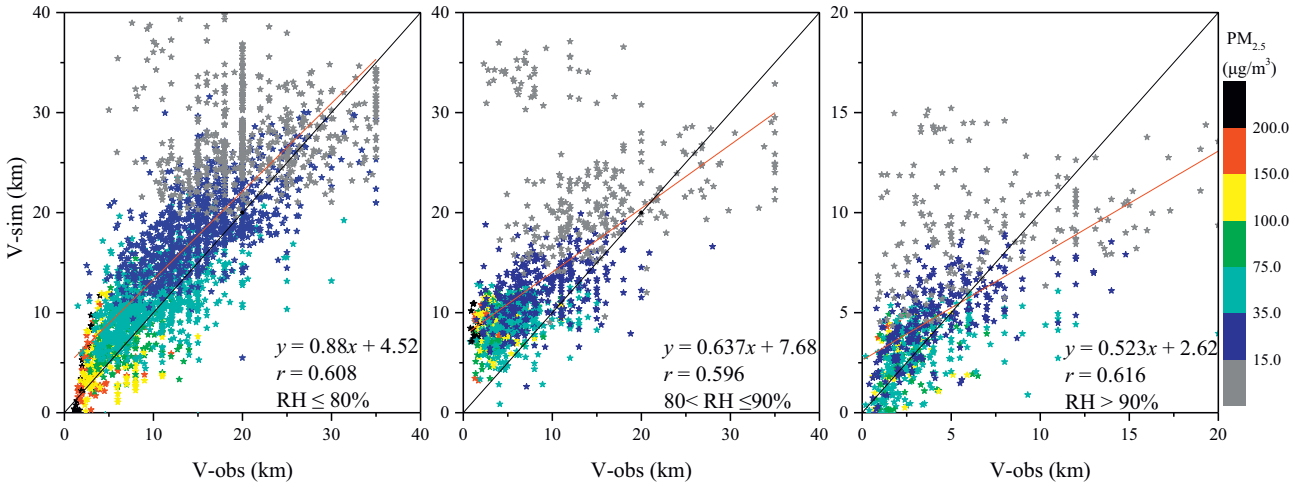

Fig. 5 – Comparison between the observed hourly visibility and regression model simulated hourly visibility during 2013.6–2014.5. (V-obs: the observed visibility; V-sim: the simulated visibility).

contributor to visibility (aside from $PM_{2.5}$ and RH) within RH of 80–90%. The importance of O_3 in the model requires further investigation. Results presented in Table 1 also suggested that temperature can affect visibility when RH > 90%. Likely, temperature affects visibility by influencing condensation of water vapor in the atmosphere.

To further verify the validity of the non-linear models combining exponential and multiple linear regressions, hourly observed visibility data from June 2013 to May 2014 were examined. Fig. 5 presents the simulated results based on equations in Table 1 vs. the observed visibility. The newly developed multiple nonlinear model improved the visibility prediction with generally higher R values compared to those based on single parameter regression model (Eq. (3)), especially under high RH (>90%) conditions (Fig. S2). A time series of daily observed visibility and daily visibility simulated by nonlinear regression model from June 2013 to May 2014 is plotted in Fig. 6. There was a high degree of consistency between model-fitted visibility and observed visibility, indicating that the newly developed model is a suitable and practical model for simulating visibility based on air quality in DQL area.

3. Conclusions

Visibility, atmospheric pollutants and meteorological variables monitored in a suburban area (DQL) of Ningbo from June 1, 2013 to May 31, 2015 were analyzed in this study. The characteristics of visibility and its affecting factors were described in detail using multiple statistical methods.

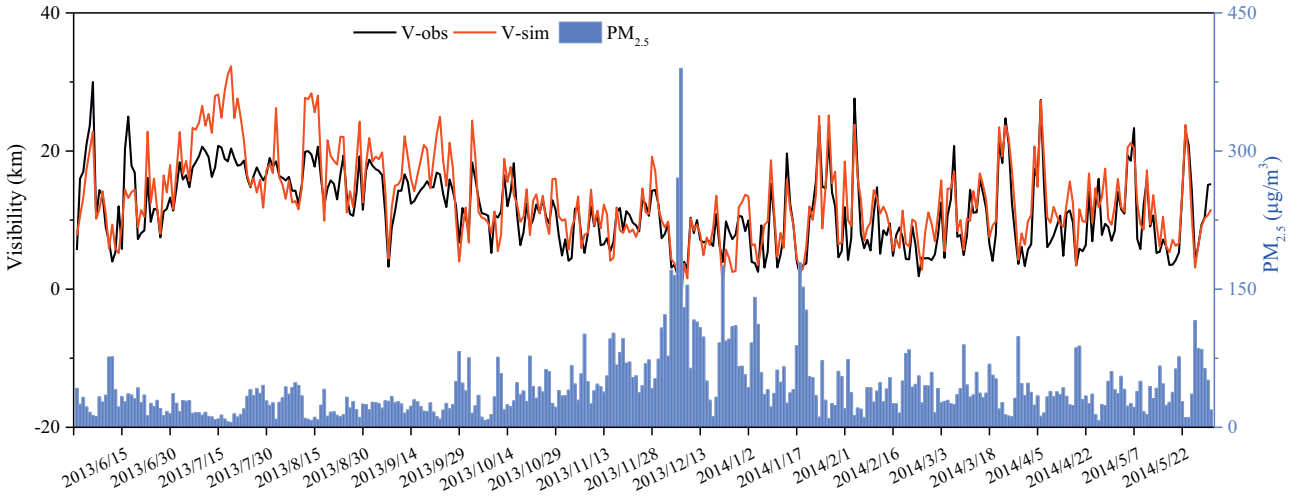

Fig. 6 – Time series of daily observed visibility and daily simulated visibility by stepwise regression equations at DQL. (V-obs: the observed visibility; V-sim: the simulated visibility).

Based on these analyses, the following conclusions can be derived:

The temporal variation of visibility in DQL during the study period demonstrated notable regional characteristics. The seasonal pattern of visibility was characterized by higher levels in spring–summer and lower levels in autumn–winter. Nearly half of all measurements of visibility were lower than 10 km, indicating poor air quality over the study region. Visibility displayed an obvious diurnal variation in each season, with the lowest and highest visibility being 7.5 km at approximately 06:00, and 15.6 km at approximately 14:00, respectively.

The results of MCA indicated that good visibility was always associated with good meteorological conditions and low levels of air pollutants, except for O_3. The results of MCA explained 66.9% necessity of the segmented studies of visibility. Based on the correlation analysis, $PM_{2.5}$, WS and relative humidity were found to have significant impacts on visibility in Ningbo. Also, model equations between visibility, PM and RH were derived, with visibility decreasing exponentially with increasing $PM_{2.5}$ concentrations in different RH ranges. Additionally, the non-linear models combining exponential with multiple linear regressions were developed to investigate the underlying relationships between visibility, air quality and meteorological conditions. The main factors which have the largest influences on visibility change under different RH ranges. Based on a comparative evaluation, the model prediction was found to be relatively accurate for this suburban area.

This study demonstrated that the correlations between visibility and air pollutants/meteorological parameters are relatively consistent and it is possible to predict visibility based on air pollutant concentrations and weather conditions in Ningbo. However, the coefficients and model fitting of other cities may differ from Ningbo due to variations in the pollution characteristics and weather conditions. In order to gain a more precise and generalized model and to simulate the visibility in other cities (such as in YRD region), a data set of multiple cities will be considered in our future work.

Acknowledgments

This work was supported by the National Natural Science Foundation of China (No. 31300435, U1405235), Science and Technology Plan Project of Ningbo City (No. 2015C110001), Natural Science Foundation of Ningbo City (No. 2015A610247), and Knowledge Innovation Program of the Chinese Academy of Sciences (No. IUEQN-2012-03). We gratefully thank Dr. Graeme W. Nicol from university of Lyon for his comments and English polishing.

Appendix A. Supplementary data

Supplementary data to this article can be found online at https://doi.org/10.1016/j.jes.2018.09.015.

REFERENCES

Cao, J.J., Wang, Q.Y., Chow, J.C., Watson, J.G., Tie, X.X., Shen, Z. X., et al., 2012. Impacts of aerosol compositions on visibility impairment in Xi'an, China. Atmos. Environ. 59, 559–566.

Chan, Y.C., Simpson, R.W., Mctainsh, G.H., Vowles, P.D., Cohen, D. D., Bailey, G.M., 1999. Source apportionment of visibility degradation problems in Brisbane (Australia) using the multiple linear regression techniques. Atmos. Environ. 33, 3237–3250.

Charlson, R.J., Schwartz, S.E., Hales, J.M., Cess, D., Coakley, J.A., Hansen, J.E., 1992. Climate forcing by anthropogenic aerosols. Science 255, 423–430.

Che, H.Z., Zhang, X.Y., Li, Y., Zhou, Z.J., Chen, Z.L., 2006. Relationship between horizontal extinction coefficient and PM_{10} concentration in Xi'an, China, during 1980–2002. Particuology 4, 327–329.

Cheng, Z., Wang, S.X., Fu, X., Watson, J.G., Jiang, J., Fu, Q., et al., 2014. Impact of biomass burning on haze pollution in the Yangtze River Delta, China; a case study in summer 2011. Atmos. Chem. Phys. 14, 4573–4585.

China Environmental Protection Ministry, 2012. GB 3095–2012 Ambient Air Quality Standards in China. Ministry of Environmental Protection and General Administration of Quality Supervision. Inspection and Quarantine of the People's Republic of China.

Deng, J.J., Wang, T.J., Jiang, Z.Q., Xie, M., Zhang, R.J., Huang, X.X., et al., 2011. Characterization of visibility and its affecting factors over Nanjing, China. Atmos. Res. 101, 681–691.

Deng, J.J., Xing, Z.Y., Zhuang, B.L., Du, K., 2014. Comparative study on long-term visibility trend and its affecting factors on both sides of the Taiwan Strait. Atmos. Res. 143, 266–278.

Du, K., Mu, C., Deng, J.J., Yuan, F., 2013. Study on atmospheric visibility variations and the impacts of meteorological parameters using high temporal resolution data: an application of environmental internet of things in China. Int. J. Sust. Dev. World 20, 238–247.

Garson, G.D., 2012. Correspondence analysis [Internet]. Statnotes: topics in multivariate analysis. Available at http://www.statisticalassociates.com/correspondenceanalysis.htm.

Hair, J.F., Anderson, R.E., Tatham, R.L., Black, W.C., 1995. Multivariate Data Analysis. fourth ed. College Division, Prentice Hall, p. 745.

He, T.F., Yang, Z.Y., Liu, T., Shen, Y.P., Fu, X.H., Qian, X.J., et al., 2016. Ambient air pollution and years of life lost in Ningbo, China. Sci. Rep. 6.

Higgs, N.T., 1991. Practical and innovative uses of correspondence analysis. Underst. Stat. 40, 183–194.

Hill, T., Lewicki, P., 2007. Statistics: Methods and Applications. Statsoft, Tulsa, p. 800.

Horvath, H., 1995. Estimation of the average visibility in Central Europe. Atmos. Environ. 29, 241–246.

Hua, Y., Chen, Z., Zhang, J.K., Wang, S.X., Jiang, J.K., Chen, D., et al., 2015. Characteristic and source apportionment of $PM_{2.5}$ during a fall heavy haze episode in the Yangtze River Delta of China. Atmos. Environ. 123, 380–391.

Jung, J., Lee, H., Kim, Y.J., Liu, X.G., Zhang, Y.H., Gu, J.W., et al., 2009. Aerosol chemistry and the effect of aerosol water content on visibility impairment and radiative forcing in Guangzhou during the 2006 Pearl River Delta campaign. J. Environ. Manag. 90, 3231–3244.

Kim, Y.J., Kim, K.W., Kim, S.D., Lee, B.K., Han, J.S., 2006. Fine particulate matter characteristics and its impact on visibility impairment at two urban sites in Korea: Seoul and Incheon. Atmos. Environ. 40, 593–605.

Kumar, R., Naja, M., Venkataramani, S., Wild, O., 2010. Variations in surface ozone at Nainital: a high-altitude site in the central Himalayas. J. Geophys. Res.-Atmos. 115, 751–763.

Lin, M., Tao, J., Chan, C.Y., Cao, J.J., Zhang, Z.S., Zhu, L.H., et al., 2012. Regression analyses between recent air quality and visibility changes in megacities at four haze regions in China. Aerosol Air Qual. Res. 12, 1049–1061.

Pudasainee, D., Sapkota, B., Shrestha, M.L., Kaga, A., Kondo, A., Inoue, Y., 2006. Ground level ozone concentrations and its association with NO_x and meteorological parameters in Kathmandu valley, Nepal. Atmos. Environ. 40, 8081–8087.

Sabetghadam, S., Ahmadi-Givi, F., 2014. Relationship of extinction coefficient, air pollution, and meteorological parameters in an urban area during 2007-2009. Environ. Sci. Pollut. Res. 21, 538–547.

Semple, D., Song, F., Gao, Y., 2012. Seasonal characteristics of ambient nitrogenoxides and ground-level ozone in metropolitan northeastern New Jersey. Atmos. Pollut. Res. 3, 247–257.

Shen, Z.X., Cao, J.J., Zhang, L.M., Qian, Z., Huang, R.J., Liu, S.X., et al., 2016. Retrieving historical ambient $PM_{2.5}$ concentrations using existing visibility measurements in Xi'an, Northwest China. Atmos. Environ. 126, 15–20.

Sourial, N., Wolfson, C., Zhu, B., Quail, J., Fletcher, J., Bergman, H., 2010. Correspondence analysis is a useful tool to uncover the relationship among categorical variables. J. Clin. Epi. 63, 638–646.

Tan, J.H., Duan, J.C., Chen, D.H., Wang, X.H., Guo, S.J., Bi, X.H., et al., 2009a. Chemical characteristics of haze during summer and winter in Guangzhou. Atmos. Res. 94, 238–245.

Tan, J.H., Duan, J.C., He, K.B., Ma, Y.L., Duan, F.K., Chen, Y., et al., 2009b. Chemical characteristics of $PM_{2.5}$ during a typical haze episode in Guangzhou. J. Environ. Sci. 21, 774–781.

Tong, L., Zhang, H.L., Yu, J., He, M.M., Xu, N.B., Zhang, J.J., et al., 2017. Characteristics of surface ozone and nitrogen oxides at urban, suburban and rural sites in Ningbo, China. Atmos. Res. 187, 57–68.

Tsai, Y.I., 2005. Atmospheric visibility trends in an urban area in Taiwan 1961–2003. Atmos. Environ. 39, 5555–5567.

Tsai, Y.I., Lin, Y.H., Lee, S.Z., 2003. Visibility variation with air qualities in the metropolitan area in southern Taiwan. Water Air Soil Pollut. 144, 19–40.

Tu, J., Xia, Z.G., Wang, H., Li, W., 2007. Temporal variations in surface ozone and its precursors and meteorological effects at an urban site in China. Atmos. Res. 85, 310–337.

Van Stan, J.T., Gay, T.E., Lewis, E.S., 2016. Use of multiple correspondence analysis (MCA) to identify interactive meteorological conditions affecting relative throughfall. J. Hydro. 533, 452–460.

Wang, Y., Zhuang, G.S., Sun, Y.L., An, Z.S., 2006. The variation of characteristics and formation mechanisms of aerosols in dust, haze, and clear days in Beijing. Atmos. Environ. 40, 6579–6591.

Wark, K., Warner, C.F., Davis, W.T., 1998. Air Pollution–Its Origin and Control. 3rd edition. Addison–Wesley, MA, United States, p. 573.

Watson, J.G., 2002. Critical review discussion-visibility: Science and regulation. J. Air Waste Manag. 52, 973–999.

Wen, C.C., Yeh, H.H., 2010. Comparative influences of airborne pollutants and meteorological parameters on atmospheric visibility and turbidity. Atmos. Res. 96, 496–509.

Xu, J., Bergin, M.H., Yu, X., Zhao, J., Carrico, C.M., Baumann, K., 2002. Measurement of aerosol chemical, physical and radiative properties in the Yangtze delta region of China. Atmos. Environ. 36, 161–173.

Xue, D., Li, C.F., Liu, Q., 2015. Visibility characteristics and the impacts of air pollutants and meteorological conditions over Shanghai, China. Environ. Monit. Assess. 187, 363–373.

Yang, L.X., Wang, D.C., Chen, S.H., Wang, Z., Zhou, Y., Zhou, X.H., et al., 2007. Influence of meteorological conditions and particulate matter on visual range impairment in Jinan, China. Sci. Total Environ. 383, 164–173.

Yu, X.N., Ma, J., An, J.L., Yuan, L., Zhu, B., Liu, D.Y., et al., 2016. Impacts of meteorological condition and aerosol chemical compositions on visibility impairment in Nanjing, China. J. Clean. Prod. 131, 112–120.

Zhang, Q.H., Zhang, J.P., Xue, H.W., 2010. The challenge of improving visibility in Beijing. Atmos. Chem. Phys. 10, 7821–7827.

Zhang, X.Y., Wang, Y.Q., Niu, T., Zhang, X.C., Gong, S.L., Zhang, Y. M., et al., 2012. Atmospheric aerosol compositions in China: spatial/temporal variability, chemical signature, regional haze distribution and comparisons with global aerosols. Atmos. Chem. Phys. 12, 779–799.

Zhao, P.S., Zhang, X.L., Xu, X.F., Zhao, X.J., 2011. Long-term visibility trends and characteristics in the region of Beijing, Tianjin, and Hebei, China. Atmos. Res. 101, 711–718.

Zheng, S., Cao, C.X., Singh, R.P., 2014. Comparison of ground based indices (API and AQI) with satellite based aerosol products. Sci. Total. Environ. 488, 398–412.